tvst

Article

Choroidal Thickness by Handheld Swept-Source Optical Coherence Tomography in Term Newborns

Laura C. Huang[1,2], Hao Zhou[3], Alex T. Legocki[2], N. Max Scoville[2], Junping Zhong[3], Leona Ding[2], Ruikang K. Wang[2,3], and Michelle T. Cabrera[1,2]

[1] Division of Pediatric Ophthalmology, Seattle Children's Hospital, Seattle, WA, USA
[2] Department of Ophthalmology, University of Washington, Seattle, WA, USA
[3] Department of Bioengineering, University of Washington, Seattle, WA, USA

Correspondence: Michelle T. Cabrera, Seattle Children's Hospital, MS OA.9.220, 4800 Sand Point Way NE, Seattle, WA 98105, USA. e-mail: cabreram@uw.edu

Received: July 29, 2020
Accepted: January 9, 2021
Published: February 17, 2021

Keywords: choroid; optical coherence tomography; infancy

Citation: Huang LC, Zhou H, Legocki AT, Scoville NM, Zhong J, Ding L, Wang RK, Cabrera MT. Choroidal thickness by handheld swept-source optical coherence tomography in term newborns. Trans Vis Sci Tech. 2021;10(2):27, https://doi.org/10.1167/tvst.10.2.27

Purpose: To describe normative values for choroidal thickness in newborns and characterize their relationship to vitreoretinal features.

Methods: Term newborns underwent awake, handheld swept-source optical coherence tomography (SS-OCT) in this prospective cohort study. An automated segmentation algorithm followed by manual adjustments measured choroidal thickness at the fovea and five perifoveal locations. Two masked, trained graders, with a third mediating disagreements, analyzed scans for vitreoretinal findings. OCT vitreoretinal findings, including dome-shaped macula, subretinal fluid, punctate hyperreflective vitreous opacities, persistent inner retinal layers, foveal ellipsoid zone, tractional and non-tractional vitreous bands, epiretinal membrane, cystoid macular edema, vessel elevation, scalloped retinal layers, hyporeflective vessels, and retinal spaces, were assessed and correlated with foveal choroidal thickness using a generalized linear mixed model.

Results: Fifty-nine eyes of 39 infants (mean gestational age, 39.5 weeks; 18 male, 46%) were included. Mean foveal choroidal thickness was 455.5 $\pm$ 93.9 µm. Choroid was thinner inferonasally (343.6 $\pm$ 106.2 µm) compared to superonasally (368.4 $\pm$ 92.9 µm; $P = 0.03$) and superotemporally (369.6 $\pm$ 100.6 µm; $P = 0.02$). Thinner foveal choroidal thickness was associated with absence of a foveal ellipsoid zone (437.1 $\pm$ 78.5 µm vs. 553.7 $\pm$ 93.9 µm; $P = 0.02$). Choroidal thickness was not significantly associated with other OCT findings.

Conclusions: We identified an association between thinner choroid and foveal immaturity. Additional study is needed to determine whether choroidal development impacts visual outcomes.

Translational Relevance: Handheld SS-OCT achieved normative measurements for choroidal thickness across the macula in term newborns, providing a foundation for future investigations into the role of choroidal development in infancy.

Introduction

The choroid is a highly vascular tissue that supplies oxygen and nutrients to the photoreceptors and the retinal pigment epithelium (RPE). The choroid has been implicated in numerous pathologies in adults, including central serous chorioretinopathy and age-related macular degeneration.[1,2] In the pediatric population, choroidal structural differences have been correlated with refractive error, birth weight, retinopathy of prematurity (ROP), and gestational age.[3–5]

Due to its location behind pigmented RPE, imaging the choroid is difficult by fluorescein angiography and conventional optical coherence tomography (OCT) technology. Spectral-domain (SD) OCT, performed at central wavelengths of 800 to 870 nm, could provide adequate resolution but is often hindered by insufficient penetration into deeper tissues and backscattering of light due to the RPE.[6,7] Advancements in OCT technology have facilitated more accurate choroidal imaging. The enhanced depth imaging SD-OCT technique brings deeper structures to the zero-delay line, enabling maximal sensitivity for signal

detection; however, these modifications may also degrade vitreoretinal details.[8] More recently, the advent of swept-source (SS) OCT allows for precise visualization of both retinal and choroidal anatomy due to a much higher rate of image acquisition, longer wavelengths in the range of 1050 to 1060 nm, and less signal roll-off.[8] Furthermore, advances in SS-OCT imaging have allowed for topographic mapping of choroidal thickness.

Given that the choroid provides blood supply to the developing retina, any variation in choroidal development in infancy may impact retinal maturity or relate to other vitreoretinal pathologic changes.[9] Handheld OCT technology has detected numerous vitreoretinal findings in both preterm and term infants that may serve as markers of retinal maturation. Persistent inner retinal layers and absent foveal ellipsoid zone are indicators of foveal immaturity in both preterm and term infants.[10–12] Vessel elevation, scalloped retinal layers, hyporeflective vessels, and retinal spaces were first described as markers of plus disease for infants with ROP[13] and may serve as general indicators of OCT retinal vascular characteristics. Punctate hyperreflective vitreous opacities[14] have also been associated with ROP in preterm infants and may relate to normal ocular development in full-term infants.[15] Structural abnormalities, including epiretinal membrane (ERM)[11] and cystoid macular edema (CME),[11] have been associated with both tractional and non-tractional vitreous bands in premature infants,[14,16] with unknown impact on choroidal thickness. Finally, subfoveal fluid[17] is a finding of unclear etiology found in roughly 15% of full-term newborns and may represent variation in normal early ocular development. To better understand normal retinal development, this study sought to utilize an investigational handheld SS-OCT device to characterize normative values for choroidal thickness in term newborns across the macula and to evaluate whether choroidal thickness correlates with other OCT vitreoretinal findings.

Methods

Study Participants

Term newborn infants in the University of Washington Maternal Infant Center were enrolled in this prospective, observational study with institutional review board approval at the University of Washington (Seattle, WA). Infants were eligible if gestational age was ≥37 weeks and infants were ≥12 hours old. Infants with substantial social barriers (such as parental drug dependence or uncertain guardianship) or known systemic disease were excluded. Infants were also excluded based on subjective determination of inadequate image quality (optic nerve or macula were not visualized or severe motion artifact interfered with accurate choroidal thickness measurements) by one of the authors (LCH). Informed consent was obtained from legal guardians after explanation of the nature and possible consequences of the study. Each infant's medical record was reviewed for gestational age, birth weight, sex, and race in order to understand demographic relationships to choroidal thickness in this population.

Study Imaging

This study utilized an investigational prototype handheld SS-OCT system developed at the University of Washington in the laboratory of one of the authors (RKW).[18] This prototype contains a swept-source laser with a central wavelength of 1051 nm, 200-kHz A-scan rate, and a spectral tuning range of 105.2 nm. This provides a measured axial resolution of approximately 6 µm in tissue and a calculated lateral resolution on the retina of approximately 16 µm (for a typically 7 × 7-mm, or 40°, field of view at 400 B-scans × 400 A-scans/B-scan and with four repeats).[18,19]

Participating infants underwent a single awake imaging session within the first 72 hours of life. Imaging was performed as previously described.[18,19] Briefly, infants were dilated with 1% phenylephrine hydrochloride and 0.2% cyclopentolate (Cyclomydril; Alcon Laboratories, Fort Worth, TX) at least 40 minutes prior to the examination. One of the authors (ATL), who was experienced in handheld OCT, imaged all infants in the supine position without an eyelid speculum or ocular contact. The eyelids were gently held open with the imager's fingers. A screen located on the probe displayed a live video of the pupil and OCT B-scan image as feedback to better localize the region of interest. Image acquisition was restricted to a maximum of 15 minutes for both eyes. The scans were performed with special attention to the posterior pole, aiming to capture the highest quality foveal and optic nerve images using multiple volume scans. OCT angiography was also performed within the time limit but was not reported in this study.

Choroidal Segmentation

To generate the three-dimensional OCT structural image, raw spectrum data were first reassembled and convolved with a phase vector obtained from calibration to eliminate a wavelength dispersion effect and

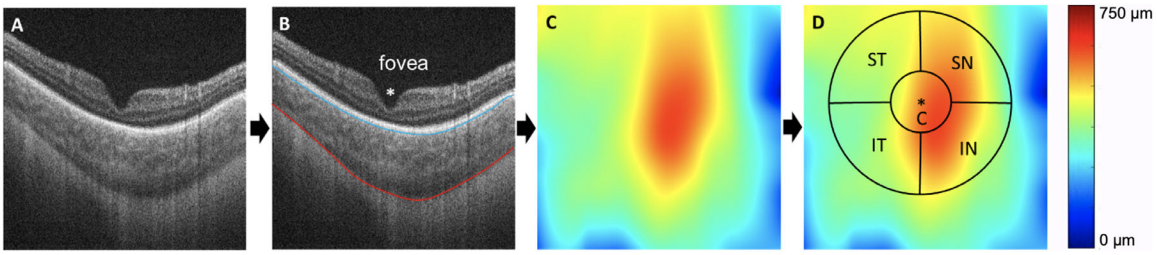

Figure 1. Steps for choroidal thickness analysis. (A) SS-OCT B-scans were obtained in awake infants. (B) Segmentation of the choroidal layer was performed using semi-automated methods. *Blue line*, Bruch's membrane segmentation; *red line*, choroidal–scleral interface segmentation; *asterisk*, foveal location. (C) En face 7 × 7-mm choroidal thickness maps were generated. (D) Choroid thickness maps were overlaid with grids for subfield analysis.

were then processed as previously described.[20] One masked, trained grader (LCH) evaluated all OCT volume scans. The highest quality scan was chosen for each eye based on subjective assessment of image resolution and centration around the optic nerve and fovea. Choroidal segmentation was carried out via an automated custom segmentation algorithm developed in a computing environment (MATLAB; MathWorks, Inc., Natick, MA) to determine the anterior and posterior choroidal boundaries (Bruch's membrane and the choroidoscleral interface, respectively). The choroidal slab was automatically segmented by an attenuation correction-assisted algorithm previously validated in a normative adult database.[21,22] Automated segmentation followed by ad hoc manual adjustments were performed by one of the authors (LCH) on all 400 B-scans from each eye using custom software. Excluding the optic nerve, en face choroidal thickness maps were generated (Fig. 1).

Due to axial length (AL) variation with gestational age, the field of view was not uniform. To compensate for these differences, AL for each infant was estimated by the infant's gestational age based on a previous normative database.[23] The corrected field of view was calculated using the following equation: corrected field of view length = infant eye AL/standard adult AL (24 mm) × system field of view length (7 mm).[24] Choroidal thickness maps were resized, and the whole field of view was normalized to 7 × 7 mm for further analysis.

In order to quantify and compare choroidal thickness, we utilized a grid resembling the Early Treatment Diabetic Retinopathy Study (ETDRS) grid.[22,25] The grid was composed of an inner circle with a 1.5-mm diameter demarcating the perifovea and an outer concentric region with a 5-mm diameter. This outer circle was divided into four subfields (superonasal, superotemporal, inferonasal, and inferotemporal) based on prior reports demonstrating choroidal thickness differences across a cross-shaped rather than an x-shaped divide (Fig. 1).[22,25,26] For each OCT volume, the location of the fovea was determined manually by analyzing B-scan images. The ETDRS-like grid was then centered at the corresponding foveal location on the choroidal thickness maps, with mean subfield thickness calculated using MATLAB software.

An average choroidal thickness map was generated by calculating the mean choroidal thickness of the whole study group. To do so, en face choroid thickness maps after scale correction of all cases were registered at the fovea (and optic nerve head, if present in the scan region). Images of right eyes were flipped and images of left eyes remained the same. The mean values of the registered maps were calculated. The 95% normal limits for mean choroidal thickness maps were estimated using 2 SDs above and below the mean at each pixel and then smoothed for the final maps. Data that were either larger than 3 SDs above the mean or smaller than 3 SDs below the mean were excluded as outliers.

Image Analysis for Vitreoretinal Features Outside the Choroid

Two trained graders (ATL, NMS) evaluated all SS-OCT volumes for several vitreoretinal findings to understand the relationship between choroidal thickness and other vitreoretinal features in this population. Disagreements were mediated by a third trained grader (MTC). OCT vitreoretinal findings graded for this study are described in Table 1. We used a more inclusive definition[27] of dome-shaped macula than recent publications due to the inability to accurately measure dome height using the handheld OCT device. All volumes were assessed for the presence of punctate hyperreflective vitreous opacities which, when present, were quantified using a semiautomated software developed at the University of Washington (https://github.com/uw-biomedical-ml/segmentations), as previously

Table 1. Definitions of Vitreoretinal Findings Evaluated in All Handheld SS-OCT Scans in Term Newborns

Vitreoretinal SS-OCT Findings*	Definition
Punctate hyperreflective vitreous opacities[14]	Hyperreflective opacities, not attached to retina, visible above background and excluding above the optic nerve†
Non-tractional vitreous bands[16]	Hyperreflective linear opacities in the vitreous, parallel to the retina, seen in ≥3 consecutive B-scan frames
Tractional vitreous bands[16]	Vitreous bands that appear to meet the retina at a steeper angle
Persistent inner retinal layers[11,12,34]	Presence of foveal retinal layers from inner to outer nuclear layers
Subretinal fluid[17,42]	Hyporeflective space between the retina and the RPE at the fovea
Foveal ellipsoid zone[10]	Presence of an ellipsoid zone at the fovea
Dome-shaped macula[27]	Retinal, RPE, and choroid convexity on both sides of the fovea
Epiretinal membrane[19]	Thick linear hyperreflectivity at the inner retina with visible separation from the retina but not overlying vessels or optic nerve
Cystoid macular edema[11,12]	Hyporeflective spaces typically present in the inner nuclear layer in and around the fovea in multiple B-scans, distorting retinal layers
Vessel elevation[13]	A spiked vessel extending beyond the retinal surface (defined as mild or severe) located >1/2 disc diameter from the optic disc
Scalloped retinal layers[13]	Scalloped inner plexiform layer (mild) or inner and outer plexiform layers (severe) located >1/2 disc diameter from the optic disc
Hyporeflective vessels[13]	Hyporeflective vessel lumen with shadowing columns found >1/2 disc diameter from the optic disc
Retinal spaces[13]	Hyporeflective spaces next to vessels that do not create shadowing

*All findings were evaluated by two trained graders with a third trained grader serving as the tiebreaker.
†We calculated the vitreous opacity ratio using semi-automated methods to quantify the punctate opacities in the foveal/parafoveal region, averaging the results of the two graders.

described.[14] Briefly, the software generated a vitreous opacity ratio, which calculated the total number of opacities over five B-scans in and around the fovea divided by total vitreous area in pixels and averaged between two graders.[14] For this part of the study, 100 B-scans per volume with 16 repeats were used to increase sensitivity to capture punctate opacities.

Statistical Analysis

Comparisons between mean choroidal thickness at varying anatomical locations were performed. Mean central foveal choroidal thickness was correlated with sex, race, birth weight, and gestational age, as well as OCT graded vitreoretinal findings, including the vitreous opacity ratio. For birth weight and gestational age, the Mann–Whitney *U* test was utilized, as these failed the Shapiro–Wilk test of normality. For all other analyses, a generalized linear mixed model was applied to account for non-independence of multiple observations per infant (two eyes). In order to assess interobserver agreement between graders for OCT vitreoretinal findings, the unweighted Cohen's kappa (κ) statistic was calculated.[28] Interobserver agreement for quantification of punctate opacities (vitreous opacity ratio) relied on the F1 score for counting opacities and the Dice coefficient for measuring vitreous area. Statistical analyses were performed using SAS 9.4 (SAS Institute, Inc., Cary, NC) and SPSS Statistics for Windows, Version 26.0 (IBM Corp., Armonk, NY). $P < 0.05$ was considered statistically significant.

Results

Fifty newborn term infants were recruited for the study, of whom 41 eyes (41%) and 11 infants (22%) were excluded due to inadequate image quality (severe motion artifact and/or no visible fovea). Of the remaining 39 infants (59 eyes), 18 were males (46%) with mean 39.5 ± 1.4 weeks gestational age and 3392.4 ± 498.9 grams birth weight. Twenty-two were white (56%), six were Asian (15%), three were Hispanic (8%), three were African American (8%), and five were classified as other (13%). Female choroid (488.2 ± 102.5 µm; $n = 34$ eyes) was thicker than male choroid (411.1 ± 57.2 µm; $n = 25$ eyes) ($P < 0.001$). Choroidal thickness varied across race and was thickest in the eyes of whites (492.7 ± 93.4 µm; $n = 34$) followed by Hispanics (453.2 ± 126.3 µm; $n = 4$), African Americans (431.1 ± 47.4 µm; $n = 5$), other (390.3 ± 28.2 µm; $n = 6$), and Asians (381.2 ± 60.1 µm; $n = 10$) ($P < 0.001$). Choroidal thickness had no significant association with birth weight ($P = 0.11$) or gestational age ($P = 0.28$) (Table 2).

Normative Values for Choroidal Thickness Across the Macula

Choroidal segmentation analysis demonstrated macular topographic variation (Table 3). Choroidal thickness at the fovea (455.5 ± 93.9 µm) was thicker than in the superonasal (368.4 ± 92.9 µm; $P = < 0.0001$), superotemporal (369.6 ± 100.6 µm; $P = <0.0001$), inferonasal (343.6 ± 87.9 µm; $P = <0.0001$), and inferotemporal (347.0 ± 106.2 µm; $P = <0.0001$) quadrants. Choroidal thickness of the perifovea (443.1 ± 91.0 µm) was thicker than in the superonasal (368.4 ± 92.9 µm; $P = <0.0001$), superotemporal (369.6 ± 100.6 µm; $P = <0.0001$), inferonasal (343.6 ± 87.9 µm; $P = <0.0001$), and inferotemporal (347.0 ± 106.2 µm; $P = <0.0001$) quadrants. The choroid was thinner inferonasally (343.6 ± 106.2 µm) compared to the superonasal (368.4 ± 92.9 µm; $P = 0.03$) and superotemporal (369.6 ± 100.6 µm; $P = 0.02$) quadrants.

Table 2. Choroidal Thickness Correlation to Demographic and Vitreoretinal Features by Handheld SS-OCT[*]

	Value	Choroidal Thickness at Fovea (μm), Mean (SD)	P[†]
Patient demographics			
Sex, *n* (%)			<0.001
Male	25 (42)	411.1 (57.2)	
Female	34 (58)	488.2 (102.5)	
Birth weight (g), mean (SD)	3392.4 (498.9)		0.11[‡]
Gestational age (wk), mean (SD)	39.5 (1.4)		0.28[‡]
Race, *n* (%)			<0.001
White	34 (58)	492.7 (93.4)	
Hispanic	4 (7)	453.2 (126.3)	
Black	5 (8)	431.1 (47.4)	
Asian	10 (17)	381.2 (60.1)	
Unknown or unavailable	6 (10)	390.3 (28.2)	
SS-OCT vitreoretinal findings, *n* (%)[§]			
Dome-shaped macula			0.27
Absent	54 (92)	459.3 (96.9)	
Present	5 (8)	415.0 (33.8)	
Subretinal fluid			0.33
Absent	49 (83)	460.9 (93.8)	
Present	10 (17)	429.4 (95.3)	
Punctate hyperreflective vitreous opacities			0.35
Absent	11 (19)	475.6 (100.5)	
Present	48 (81)	450.9 (92.9)	
Persistent inner retinal layers at fovea			0.29
Absent	4 (7)	490.9 (76.1)	
Present	55 (93)	452.9 (95.2)	
Foveal ellipsoid zone[‖]			0.02
Absent	39 (80)	437.1 (78.5)	
Present	10 (20)	553.7 (93.9)	
Tractional vitreous bands			0.20
Absent	53 (90)	463.5 (94.6)	
Present	6 (10)	384.7 (51.1)	
Epiretinal membrane			0.98
Absent	56 (95)	456.0 (96.4)	
Present	3 (5)	446.5 (14.0)	
Cystoid macular edema			0.92
Absent	57 (97)	458.4 (94.1)	
Present	2 (3)	372.9 (44.9)	
Vessel elevation			0.50
Absent	21 (36)	406.4 (57.1)	
Present, inner	31 (52)	476.3 (97.3)	
Present, outer	7 (12)	510.7 (113.5)	
Scalloped retinal layers			0.19
Absent	28 (47)	463.3 (84.7)	
Present, inner	14 (24)	440.1 (97.5)	
Present, outer	17 (29)	455.5 (108.9)	

[*]Fifty-nine eyes of 39 infants.

[†]A generalized linear mixed model was applied to these analyses to account for non-independence of two eyes sampled per infant.

[‡]Analyses to determine *P* values were performed for the continuous variables of birth weight and gestational age.

[§]All findings were evaluated by two trained graders with a third trained grader serving as the tiebreaker.

[‖]For the foveal ellipsoid zone, $n = 49$ eyes, as the presence of an ellipsoid zone at the fovea was unknown in 10 patients due to subretinal fluid.

Table 3. Normative Values of Choroidal Thickness in the Fovea, Perifovea, and Across the Macula Among 59 Eyes of 39 Full-Term Newborns

Location*	Choroidal Thickness (µm), Mean (SD)
Fovea	455.5 (93.9)
Central (1.5-mm-diameter circle)	443.1 (91.0)
Superonasal	368.4 (92.9)
Superotemporal	369.6 (100.6)
Inferotemporal	347.0 (106.2)
Inferonasal	343.6 (87.9)

*ETDRS-like grid of macular regions (see Fig. 1).

An average choroidal thickness map was generated by calculating the mean choroidal thickness of the whole study group (Fig. 3).

Frequency of Vitreoretinal OCT Abnormalities and Association With Choroidal Thickness

Vitreoretinal findings by handheld SS-OCT demonstrated that a majority of term newborn eyes had persistent inner retinal layers at the fovea (55/59, 93.2%), absence of a foveal ellipsoid zone (39/49, 79.6%), vessel elevation (38/59, 64.4%), and scalloped retinal layers (31/59, 52.5%). A majority of patients also had punctate hyperreflective vitreous opacities (48/59, 81.4%); five of those 48 patients (10.4%) were excluded from vitreous opacity ratio analysis due to a lack of 100 B-scans per volume. The vitreous opacity ratio in the remaining 43 eyes was mean $6.1 \times 10^{-6} \pm 1.6 \times 10^{-5}$. An F1 score for agreement in grading opacities was 0.85 ± 0.19, and the Dice coefficient for agreement in vitreous segmentation was 0.99 ± 0.003. A minority of infants had subretinal fluid (10/59, 16.9%), tractional vitreous bands (6/59, 10.2%), dome-shaped macula (5/59, 8.5%), ERM (3/56, 5.4%), CME (2/59, 3.4%), and retinal spaces (1/59, 1.7%) (Table 2). The presence of an ellipsoid zone at the fovea was unknown in 10 patients due to subretinal fluid. There were no eyes in our study that had non-tractional vitreous bands or hyporeflective vessels. Cohen's κ statistic[28] for agreement by OCT graders for all vitreoretinal findings except for vessel elevation and scalloped retina (findings with subgradings of mild and severe) was 0.63 (95% confidence interval [CI], 0.47–0.75), indicating a substantial agreement. Including the two findings of vessel elevation and scalloped retina, where opportunities for disagreement in subgradings were more frequent, the κ statistic decreased (0.48; 95% CI, 0.25–0.66) to moderate agreement.

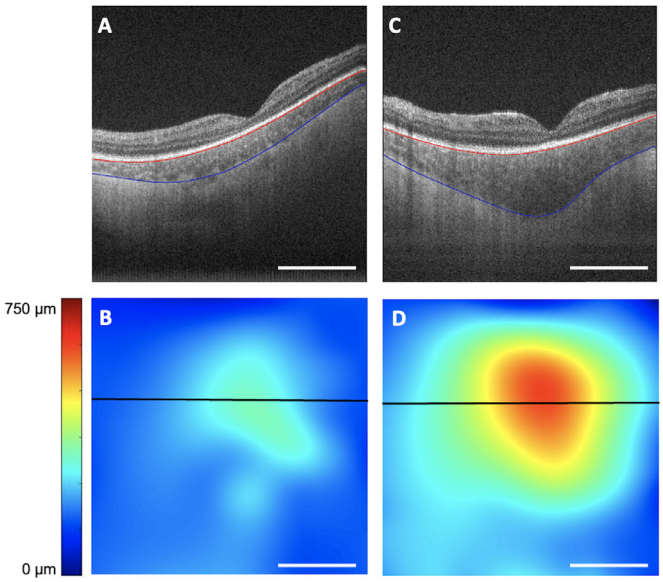

Figure 2. Choroidal thickness with and without a foveal ellipsoid zone. (A) SS-OCT of a newborn without a foveal ellipsoid zone present. (B) Corresponding choroidal thickness map (foveal choroidal thickness of 329 µm) with the associated color map in microns. (C) SS-OCT of a newborn with a foveal ellipsoid zone present. (D) Corresponding choroidal thickness map (foveal choroidal thickness of 626 µm). *Scale bar*: 2 mm.

Absent foveal ellipsoid zone was associated with thinner choroid at the fovea (437.1 ± 78.5 µm) compared to eyes with a foveal ellipsoid zone (553.7 ± 93.9 µm; $P = 0.02$) (Fig. 2). Choroidal thickness had no significant association with dome-shaped macula ($P = 0.27$), subretinal fluid ($P = 0.33$), punctate hyperreflective vitreous opacities ($P = 0.35$), persistent inner retinal layers at the fovea ($P = 0.29$), tractional vitreous bands ($P = 0.20$), ERM ($P = 0.98$), CME ($P = 0.92$), vessel elevation ($P = 0.50$), or scalloped retinal layers ($P = 0.19$) (Table 2).

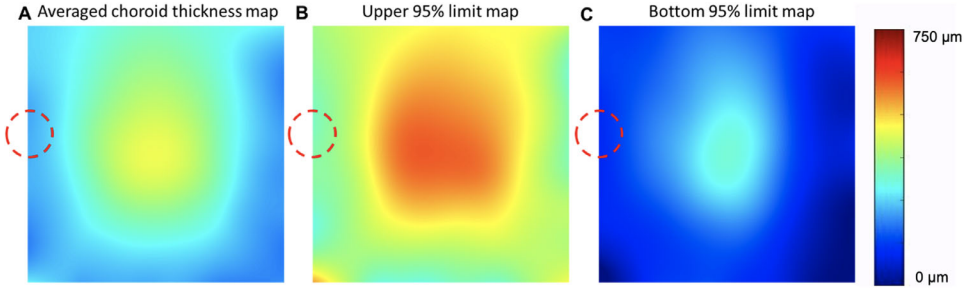

Figure 3. (A) Averaged choroidal thickness map of all infant eyes, reversing left eyes to match the right eye orientation. (B) Upper 95% limit map of choroid thickness. (C) Bottom 95% limit map of choroid thickness. *Dashed circle* indicates the location of the optic nerve head.

Discussion

To our knowledge, this paper is the first to utilize SS-OCT to capture choroidal thickness at multiple sites across the infant macula (PubMed Mesh search terms: choroid AND optical coherence tomography AND infants OR newborn OR pediatric). Using an investigational handheld SS-OCT device, this study provides normative measurements of choroidal thickness in term infants, confirming topographic variation across the macula[3,29] and demonstrating a significant association between thin choroid and foveal immaturity.

Our results show that average choroidal thickness is significantly thinner inferonasal to the fovea compared to superonasally and superotemporally. This is consistent with prior data in emmetropic children and adults,[25,29] although this differs from previous studies in infants.[6,30] Our findings utilized three-dimensional volumetric measurements and topographic mapping to analyze numerous locations across a large macular area compared to prior infant studies that utilized single B-scan measurements for each area, which were prone to sampling error.[6,30] Therefore, this study may have better elucidated the topographic variation present in infants. Previous hypotheses for the nasal–temporal choroidal asymmetry include embryologic closure of the inferior fetal fissure[31] and watershed zones within the choroidal vasculature created by the posterior ciliary arteries.[32] Topographic choroidal asymmetry was previously found to be more pronounced in myopic children, and the choroid has been implicated in refractive error development.[3] The impact of the choroid on myopia may be related to choroidal structural changes during emmetropization or choroidal release of growth factors that regulate scleral elongation.[33] Further long-term study is needed to demonstrate whether more pronounced topographic variation in infancy impacts refractive outcomes.

The present study revealed an absent foveal ellipsoid zone in 79.6% of term newborns, which is a higher rate than previously reported by Vajzovic et al. (53.2%).[34] The association between a thinner choroid and absent foveal ellipsoid zone supports prior studies suggesting that choroidal and retinal development are closely linked.[35,36] Animal models have demonstrated the need for a high rate of choroidal blood flow to meet the metabolic demands of photoreceptor inner segments,[35] and subsequent photoreceptor loss that occurs with choroidal involution supports that relationship.[36] Prior studies have also identified an absent foveal ellipsoid zone and thinner choroid in preterm and ex-preterm infants after birth, suggesting that delayed maturation during a critical period in ocular development persists postnatally.[4,6,10,30] These structural alterations may contribute to decreased vision in former preterm infants; thinner choroid has been associated with worse visual acuity in this population.[4,29] Nonetheless, the high prevalence of these findings among healthy term newborns in the present study makes significant visual impact for this population unlikely, although milder effects on visual outcomes are possible.

Our analysis of various OCT vitreoretinal findings in a population of term infants is consistent with findings in the literature. As CME, ERM, and vitreous bands are hypothesized to be related to either intraocular vascular endothelial growth factor levels or mechanical tractional forces on the macula, or both,[12,37,38] we were not surprised to find only a small number of eyes in our population that had these structural findings. In contrast, the Vascular Abnormality Score by OCT,[13] a criterion that initially described retinal vascular characteristics in the premature population, demonstrated that a majority of term infant eyes had vessel elevation and scalloped retinal layers. We attribute these changes to normal growth and dilation of the retinal vasculature with age, even though these findings are associated pathology in the preterm population.[39] Although

punctate hyperreflective vitreous opacities can correlate with the presence and severity of ROP in preterm infants,[14,40] these findings may simply represent vitreous debris[15] in term newborns. Finally, the etiology of subretinal fluid occurring in term infants is not well understood in the absence of maternal hypertension or pre-eclampsia.[17,41,42] Although choroidal thickening, or the pachychoroid spectrum,[43] has been implicated in subretinal fluid associated with central serous chorioretinopathy, we did not find an association between choroidal thickness and subretinal fluid in our population.

Our newborn infants demonstrated a thicker choroid in females and Caucasians. These findings may point to social determinants of health favoring Caucasians for chorioretinal development, although the role of ethnicity and choroidal thickness is not well characterized. Additionally, our study population had a low number of non-Caucasian Hispanic and African American participants, limiting the power of analysis for these groups. Only one study previously assessed infant choroidal thickness with regard to demographics; the authors found no significant difference in choroidal thickness between males and females, but choroid was also thicker in Caucasians (compared to Hispanics).[30] These results are consistent with prior reports in young adults[29] but differ from a study in myopic adults that found that Asians and Caucasians had thinner nasal choroid than African Americans.[44] Additional studies have suggested a thicker choroid in males,[45,46] although others have demonstrated no difference in relation to sex.[47] Variable myopia prevalence between groups may be a confounder.

This study is limited by a single-center analysis of one population. Although the kappa agreement between graders for analysis of OCT findings was mostly substantial, the confidence intervals were wide; therefore, correlations of choroidal thickness with OCT anatomical findings were imperfect. The timing of image capture occurred in the afternoon, generally within a 4-hour period, but diurnal variation in choroidal thickness has previously been reported.[48] We only captured images at one time point within the first 72 hours of life, potentially missing later changes. In awake, uncooperative newborns, we were unable to quantify more detailed morphology of choroidal vascular structure, such as dilated choroidal vessels in Haller's layer and stromal areas, as described in a recent adult choroidal OCT analysis.[2] Another limitation of the analysis is the likely overestimation of choroidal thickness in peripheral curved areas, where the measured distance between Bruch's membrane and the choroid–sclera–interface is distorted. This effect is minimized by a relatively small (5-mm circle) subfield analysis. Further correction of choroidal thickness in three-dimensional analysis is under exploration and will be necessary for widefield analysis. Nonetheless, this study used newer SS-OCT technology to examine the choroid in the term newborn population, which has been rarely studied. Use of an automated algorithm followed by careful manual segmentation maximized measurement accuracy.

Conclusions

This study demonstrated the feasibility of handheld SS-OCT to assess choroidal thickness in awake infants. Through a semi-automated choroidal segmentation algorithm, our normative measurements for choroidal thickness confirm that thinner inferonasal choroid seen in adults is also present in infancy. The association between thinner choroid and absent foveal ellipsoid zone supports a relationship between choroidal and outer retinal development. Visual and refractive outcomes for this group deserve further study.

Acknowledgments

Phanith Touch, a University of Washington medical student, contributed statistical analysis and computational expertise to calculate the vitreous opacity ratios and their interobserver agreement. He was not financially compensated for his contribution.

Supported by a core grant from the National Institutes of Health (EY 001730) and an unrestricted grant from Research to Prevent Blindness to the Department of Ophthalmology at the University of Washington.

Disclosure: **L.C. Huang**, None; **H. Zhou**, None; **A.T. Legocki**, None; **N.M. Scoville**, None; **J. Zhong**, None; **L. Ding**, None; **R.K. Wang**, None; **M.T. Cabrera**, None

References

1. Gattoussi S, Cougnard-Grégoire A, Korobelnik JF, et al. Choroidal thickness, vascular factors, and age-related macular degeneration: the ALIENOR study. *Retina*. 2019;39(1):34–43.
2. Lee M, Lee H, Kim HC, Chung H. Changes in stromal and luminal areas of the choroid in pachychoroid diseases: insights into the pathophysiology of pachychoroid diseases. *Invest Ophthalmol Vis Sci*. 2018;59(12):4896–4908.

3. Read SA, Collins MJ, Vincent SJ, Alonso-Caneiro D. Choroidal thickness in myopic and nonmyopic children assessed with enhanced depth imaging optical coherence tomography. *Invest Ophthalmol Vis Sci*. 2013;54(12):7578–7586.
4. Bowl W, Bowl M, Schweinfurth S, et al. Choroidal thickness with swept-source optical coherence tomography versus foveal morphology in young children with a history of prematurity. *Ophthalmic Res*. 2018;60(4):205–213.
5. Park KA, Oh SY. Analysis of spectral-domain optical coherence tomography in preterm children: retinal layer thickness and choroidal thickness profiles. *Invest Ophthalmol Vis Sci*. 2012;53(11):7201–7207.
6. Erol MK, Coban DT, Ozdemir O, Dogan B, Tunay ZO, Bulut M. Choroidal thickness in infants with retinopathy of prematurity. *Retina*. 2016;36(6):1191–1198.
7. Miller AR, Roisman L, Zhang Q, et al. Comparison between spectral-domain and swept-source optical coherence tomography angiographic imaging of choroidal neovascularization. *Invest Ophthalmol Vis Sci*. 2017;58(3):1499–1505.
8. Adhi M, Liu JJ, Qavi AH, et al. Choroidal analysis in healthy eyes using swept-source optical coherence tomography compared to spectral domain optical coherence tomography. *Am J Ophthalmol*. 2014;157(6):1272–1281.e1.
9. Saint-Geniez M, D'Amore PA. Development and pathology of the hyaloid, choroidal and retinal vasculature. *Int J Dev Biol*. 2004;48(8-9):1045–1058.
10. Vajzovic L, Rothman AL, Tran-Viet D, Cabrera MT, Freedman SF, Toth CA. Delay in retinal photoreceptor development in very preterm compared to term infants. *Invest Ophthalmol Vis Sci*. 2015;56(2):908–913.
11. Dubis AM, Subramaniam CD, Godara P, Carroll J, Costakos DM. Subclinical macular findings in infants screened for retinopathy of prematurity with spectral-domain optical coherence tomography. *Ophthalmology*. 2013;120(8):1665–1671.
12. Maldonado RS, O'Connell RV, Sarin N, et al. Dynamics of human foveal development after premature birth. *Ophthalmology*. 2011;118(12):2315–2325.
13. Maldonado RS, Yuan E, Tran-Viet D, et al. Three-dimensional assessment of vascular and perivascular characteristics in subjects with retinopathy of prematurity. *Ophthalmology*. 2014;121(6):1289–1296.
14. Legocki AT, Zepeda EM, Gillette TB, et al. Vitreous findings by handheld spectral domain optical coherence tomography correlate with retinopathy of prematurity severity. *Ophthalmol Retina*. 2020;4(10):1008–1015.
15. Finn AP, House RJ, Hsu ST, et al. Hyperreflective vitreous opacities on optical coherence tomography in a patient with bilateral retinoblastoma. *Ophthalmic Surg Lasers Imaging Retina*. 2019;50(1):50–52.
16. Zepeda EM, Shariff A, Gillette TB, et al. Vitreous bands identified by handheld spectral-domain optical coherence tomography among premature infants. *JAMA Ophthalmol*. 2018;136(7):753–758.
17. Cabrera MT, Maldonado RS, Toth CA, et al. Subfoveal fluid in healthy full-term newborns observed by handheld spectral-domain optical coherence tomography. *Am J Ophthalmol*. 2012;153(1):167–175.e3.
18. Song S, Zhou K, Xu JJ, Zhang Q, Lyu S, Wang R. Development of a clinical prototype of a miniature hand-held optical coherence tomography probe for prematurity and pediatric ophthalmic imaging. *Biomed Opt Express*. 2019;10(5):2383–2398.
19. Moshiri Y, Legocki AT, Zhou K, et al. Handheld swept-source optical coherence tomography with angiography in awake premature neonates. *Quant Imaging Med Surg*. 2019;9(9):1495–1502.
20. Wang RK, Ma Z. A practical approach to eliminate autocorrelation artefacts for volume-rate spectral domain optical coherence tomography. *Phys Med Biol*. 2006;51(12):3231–3239.
21. Zhou H, Chu Z, Zhang Q, et al. Attenuation correction assisted automatic segmentation for assessing choroidal thickness and vasculature with swept-source OCT. *Biomed Opt Express*. 2018;9(12):6067–6080.
22. Zhou H, Dai Y, Shi Y, et al. Age-related changes in choroidal thickness and the volume of vessels and stroma using swept-source OCT and fully automated algorithms. *Ophthalmol Retina*. 2020;4(2):204–215.
23. Cook A, White S, Batterbury M, Clark D. Ocular growth and refractive error development in premature infants with or without retinopathy of prematurity. *Invest Ophthalmol Vis Sci*. 2008;49(12):5199–5207.
24. Maldonado RS, Izatt JA, Sarin N, et al. Optimizing hand-held spectral domain optical coherence tomography imaging for neonates, infants, and children. *Invest Ophthalmol Vis Sci*. 2010;51(5):2678–2685.
25. Zheng F, Gregori G, Schaal KB, et al. Choroidal thickness and choroidal vessel density in nonexudative age-related macular degeneration using swept-source optical coherence tomography

imaging. *Invest Ophthalmol Vis Sci*. 2016;57(14):6256–6264.
26. Wang J, Gao X, Huang W, et al. Swept-source optical coherence tomography imaging of macular retinal and choroidal structures in healthy eyes. *BMC Ophthalmol*. 2015;15:122.
27. Gaucher D, Erginay A, Lecleire-Collet A, et al. Dome-shaped macula in eyes with myopic posterior staphyloma. *Am J Ophthalmol*. 2008;145(5):909–914.e1.
28. Cohen J. A coefficient of agreement for nominal scales. *Educ Psychol Meas*. 1960;20(1):37–46.
29. Lee SS, Lingham G, Alonso-Caneiro D, et al. Choroidal thickness in young adults and its association with visual acuity. *Am J Ophthalmol*. 2020;214:40–51.
30. Moreno TA, O'Connell RV, Chiu SJ, et al. Choroid development and feasibility of choroidal imaging in the preterm and term infants utilizing SD-OCT. *Invest Ophthalmol Vis Sci*. 2013;54(6):4140–4147.
31. Ikuno Y, Kawaguchi K, Nouchi T, Yasuno Y. Choroidal thickness in healthy Japanese subjects. *Invest Ophthalmol Vis Sci*. 2010;51(4):2173–2176.
32. Hayreh SS. In vivo choroidal circulation and its watershed zones. *Eye (Lond)*. 1990;4(pt 2):273–289.
33. Wallman J, Wildsoet C, Xu A, et al. Moving the retina: choroidal modulation of refractive state. *Vision Res*. 1995;35(1):37–50.
34. Vajzovic L, Hendrickson AE, O'Connell RV, et al. Maturation of the human fovea: correlation of spectral-domain optical coherence tomography findings with histology. *Am J Ophthalmol*. 2012;154(5):779–789.e2.
35. Linsenmeier R. Metabolic dependence of photoreceptors on the choroid in the normal and detached retina. *Invest Ophthalmol Vis Sci*. 2000;41(10):3117–3123.
36. Shao Z, Dorfman AL, Seshadri S, et al. Choroidal involution is a key component of oxygen-induced retinopathy. *Invest Ophthalmol Vis Sci*. 2011;52(9):6238–6248.
37. Vinekar A, Avadhani K, Sivakumar M, et al. Understanding clinically undetected macular changes in early retinopathy of prematurity on spectral domain optical coherence tomography. *Invest Ophthalmol Vis Sci*. 2011;52(8):5183–5188.
38. Vinekar A, Mangalesh S, Jayadev C, et al. Macular edema in Asian Indian premature infants with retinopathy of prematurity: impact on visual acuity and refractive status after 1-year. *Indian J Ophthalmol*. 2015;63(5):432–437.
39. Kandasamy Y, Smith R, Wright IM. Retinal microvasculature measurements in full-term newborn infants. *Microvasc Res*. 2011;82(3):381–384.
40. Lee AC, Maldonado RS, Sarin N, et al. Macular features from spectral-domain optical coherence tomography as an adjunct to indirect ophthalmoscopy in retinopathy of prematurity. *Retina*. 2011;31(8):1470–1482.
41. Sihota R, Bose S, Paul AH. The neonatal fundus in maternal toxemia. *J Pediatr Ophthalmol Strabismus*. 1989;26(6):281–284.
42. Cabrera MT, O'Connell RV, Toth CA, et al. Macular findings in healthy full-term Hispanic newborns observed by hand-held spectral-domain optical coherence tomography. *Ophthalmic Surg Lasers Imaging Retina*. 2013;44(5):448–454.
43. Cheung CMG, Lee WK, Koizumi H, Dansingani K, Lai TYY, Freund KB. Pachychoroid disease. *Eye (Lond)*. 2019;33(1):14–33.
44. Harb E, Hyman L, Gwiazda J, et al. Choroidal thickness profiles in myopic eyes of young adults in the correction of myopia evaluation trial cohort. *Am J Ophthalmol*. 2015;160(1):62–71.e2.
45. Li XQ, Larsen M, Munch IC. Subfoveal choroidal thickness in relation to sex and axial length in 93 Danish university students. *Invest Ophthalmol Vis Sci*. 2011;52(11):8438–8441.
46. Shao L, Xu L, Wei WB, et al. Visual acuity and subfoveal choroidal thickness: the Beijing Eye Study. *Am J Ophthalmol*. 2014;158(4):702–709.e1.
47. Ruiz-Medrano J, Flores-Moreno I, Peña-García P, Montero JA, Duker JS, Ruiz-Moreno JM. Macular choroidal thickness profile in a healthy population measured by swept-source optical coherence tomography. *Invest Ophthalmol Vis Sci*. 2014;55(6):3532–3542.
48. Tan CS, Ouyang Y, Ruiz H, Sadda SR. Diurnal variation of choroidal thickness in normal, healthy subjects measured by spectral domain optical coherence tomography. *Invest Ophthalmol Vis Sci*. 2012;53(1):261–266.